

Binary systems of recoiling extreme Kerr black holes

V. S. Manko,[†] E. Ruiz[‡] and M. B. Sadovnikova[‡]

[†]*Departamento de Física, Centro de Investigación y de Estudios Avanzados del IPN, A.P. 14-740, 07000 Ciudad de México, Mexico*

[‡]*Instituto Universitario de Física Fundamental y Matemáticas, Universidad de Salamanca, 37008 Salamanca, Spain*

[‡]*Department of Quantum Statistics and Field Theory, Lomonosov Moscow State University, Moscow 119899, Russia*

In the present paper the repulsion of two extreme Kerr black holes arising from their spin-spin interaction is analyzed within the framework of special subfamilies of the well-known Kinnersley-Chitre solution. The binary configurations of both equal and nonequal extreme repelling black holes are considered.

PACS numbers: 04.20.Jb, 04.70.Bw, 97.60.Lf

I. INTRODUCTION

In a recent paper [1] the possibility of the repulsion of two equal subextreme Kerr black holes due to their spin-spin interaction has been discovered within the framework of the extended solitonic spacetimes [2, 3]. Since one may reasonably suppose that the repulsion effect could be not less, but probably even stronger, in the case of extreme constituents, it would certainly be of interest to supplement the research reported in [1] with the study of the binary configurations composed of extreme Kerr black holes. Such configurations naturally arise, taking into account that the extreme limit of the usual double-Kerr metric [4] is given by the well-known Kinnersley-Chitre solution [5], as special subfamilies of the latter solution describing two extreme black holes separated by a massless strut, and these were first identified and discussed in the paper [6]. In a later work [7] the binary systems of extreme black holes were analyzed in more detail, and it might be noted that we overlooked the repulsion effect in the second subfamily from [7], being convinced that the interaction force in that subfamily had to be a positive quantity. At the same time, we did not pay much attention to the repulsion of black holes in one very special subcase of the Kinnersley-Chitre solution analyzed in [7] since its binary configurations had the ratio of total angular momentum to total mass analogous to the one characterizing a single hyperextreme Kerr source [8], i.e. $|J|/M^2 > 1$, which looked to us very exotic.

The objective of the present paper, in light of the aforementioned discovery of the black hole repulsion, is to single out and discuss the previously overlooked binary configurations of both equal and nonequal *repelling extreme* Kerr black holes that arise from the Kinnersley-Chitre solution. In particular, we are going to give a novel representation of the metric function ω for the binary systems with struts which is simpler than the one considered in [6, 7] and makes evident the presence of the axis between the constituents; we will also derive concise analytic expressions for the interaction force and for the norm of the axial Killing vector. The application of the latter expression to the analysis of the geometry around the extreme sources will allow us to obtain important information about the characteristic features of the physically meaningful configurations of repelling black holes endowed with positive masses.

II. REPULSION OF TWO IDENTICAL EXTREME KERR BLACK HOLES

The first subfamily of the Kinnersley-Chitre solution that we are going to consider describes *identical* extreme corotating Kerr black holes separated by a massless strut. This subfamily was identified in [6] and it represents the extreme limit of the solution [1]. Its Ernst complex potential [9] is determined by the expression [6]

$$\begin{aligned}\mathcal{E} &= (A - B)/(A + B), \\ A &= p^2(x^4 - 1) + q^2(y^4 - 1) - \beta^2(x^2 - y^2)^2 - 2ixy[pq(x^2 - y^2) + \beta(x^2 + y^2 - 2)], \\ B &= 2[\beta(qx + ipy)(x^2 - y^2) + px(x^2 - 1) + iqy(y^2 - 1)],\end{aligned}\tag{1}$$

where

$$\beta = \frac{1}{2p}[\Delta_S + q(1 + p)], \quad \Delta_S = \sqrt{(1 + p)(1 + 3p^2 + pq^2)},\tag{2}$$

and the real parameters p and q are subject to the constraint $p^2 + q^2 = 1$. The prolate spheroidal coordinates x and y are related to the Weyl-Papapetrou cylindrical coordinates ρ and z by the formulas

$$x = \frac{1}{2\kappa}(r_+ + r_-), \quad y = \frac{1}{2\kappa}(r_+ - r_-), \quad r_{\pm} = \sqrt{\rho^2 + (z \pm \kappa)^2}, \quad (3)$$

κ being a positive real constant; the inverse transformation is

$$\rho = \kappa\sqrt{(x^2 - 1)(1 - y^2)}, \quad z = \kappa xy. \quad (4)$$

On the symmetry axis defined by the points $\{\rho = 0, -\infty < z < +\infty\}$, potential (1) takes the form (for $z > \kappa$)

$$\begin{aligned} \mathcal{E}(\rho = 0, z) &= e_-/e_+, \\ e_{\pm} &= (p^2 - \beta^2)z^2 + 2\kappa[\pm(p + q\beta) - i(pq + \beta)]z + \kappa^2(p^2 + \beta^2 \pm 2ip\beta). \end{aligned} \quad (5)$$

The corresponding metric functions f , γ and ω entering the line element

$$ds^2 = \kappa^2 f^{-1} \left[e^{2\gamma}(x^2 - y^2) \left(\frac{dx^2}{x^2 - 1} + \frac{dy^2}{1 - y^2} \right) + (x^2 - 1)(1 - y^2)d\varphi^2 \right] - f(dt - \omega d\varphi)^2, \quad (6)$$

are given by the expressions

$$\begin{aligned} f &= \frac{E}{D}, \quad e^{2\gamma} = \frac{E}{K_0^2(x^2 - y^2)^4}, \quad \omega = \frac{\kappa(x - 1)(y^2 - 1)F}{E}, \\ E &= \mu^2 + (x^2 - 1)(y^2 - 1)\sigma^2, \\ D &= E + \mu\nu - (x - 1)(y^2 - 1)\sigma\tau, \\ F &= (x + 1)\sigma\nu + \mu\tau, \\ \mu &= p^2(x^2 - 1)^2 + q^2(y^2 - 1)^2 - \beta^2(x^2 - y^2)^2, \\ \sigma &= 2[pq(x^2 - y^2) + \beta(x^2 + y^2)], \\ \nu &= (4/K_0)\{K_0[p(x^2 + 1) + 2x^2] + K_0q\beta x(x^2 - y^2) - 2p^2\beta^2(x^2 - y^2) \\ &\quad + 4\beta(pq + \beta)x^2\}, \\ \tau &= \frac{4}{p^2 - q^2}\{(p^2 - q^2)[q(x + y^2) + p\beta(x^2 - y^2)] - (p\beta - q - 2pq)(x + 1)\}, \\ K_0 &= p^2 - \beta^2, \end{aligned} \quad (7)$$

where the novel form of ω contains the factor $(x - 1)$ explicitly, which means that ω vanishes when $x = 1$, i.e. on the intermediate ($|z| < \kappa$) part of the symmetry axis (see Fig. 1). This in turn implies that the latter portion of the axis is a strut [10, 11] – a conical angle deficit (or excess) defined by the axis value of the metric function γ .

The Komar [12] mass M and angular momentum J of each extreme Kerr constituent are given by the formulas

$$M = \frac{\kappa(p + q\beta)}{p^2 - \beta^2}, \quad J = \frac{M[2(pq + \beta)M + \kappa p\beta]}{p + q\beta}, \quad (8)$$

so that the angular momentum-mass ratio has the form

$$\delta_S \equiv \frac{J}{M^2} = \frac{1}{2}[(2 - p)\Delta_S - pq(3 - p)], \quad (9)$$

while the total values M_T and J_T are just twice the respective individual quantities: $M_T = 2M$ and $J_T = 2J$. In the paper [6] it was established that there are two parameter ranges at which M takes positive values, namely,

$$-\frac{1}{\sqrt{2}} < p < 0, \quad q > 0 \quad \text{and} \quad 0 < p < \frac{1}{\sqrt{2}}, \quad q < 0, \quad (10)$$

and these sets of parameters define, as will be seen below, two physically distinct binary configurations of extreme identical Kerr black holes, the first one (with negative p) describing a pair of black holes *attracting* each other, and the

second configuration (with positive p) describing a pair of *repelling* black holes. Indeed, the interaction force between two constituents is determined by the formula [11, 13]

$$\mathcal{F} = \frac{1}{4} (e^{-\gamma_0} - 1), \quad (11)$$

where γ_0 denotes the value of the metric function γ on the part of the axis separating the black holes. Then for both of the aforementioned subfamilies, formulas (7) yield the same simple expression

$$\mathcal{F} = \frac{p^2 - q^2}{4(q^2 - \beta^2)}, \quad (12)$$

and the plots in Fig. 2 show that \mathcal{F} takes positive values in the case of the first subfamily, and negative values in the case of the second subfamily of binary configurations. Therefore, in the systems with $p < 0$, gravitational attraction overcomes spin-spin repulsion, while in the systems with $p > 0$, spin-spin repulsion overcomes gravitational attraction, which confirms our above interpretations given to the two subfamilies.

An important point to emphasize here is that $1 < \delta_S < 2$ independently of whether a binary configuration represents attracting or repelling black holes, as it follows from the plots in Fig. 3. This means, on the one hand, that the ratio δ_S of all extreme black holes in both subfamilies exceeds the analogous value (equal to 1) of a single extreme Kerr black hole, and, on the other hand, that there are configurations of attracting and repelling extreme black holes sharing any prescribed particular value of δ_S . The latter might look strange at first glance but actually has a simple explanation – the configurations from different subfamilies possessing the same δ_S and the same coordinate separation distance 2κ will have different masses, the repelling black holes carrying the larger mass, which would be physically equivalent to having two binary systems with the same δ_S and masses but different separation distances, the shorter distance obviously corresponding to the repelling black holes. For example, it is easy to see that if $\delta_S = 1.4$ and $\kappa = 2$, then $p \simeq 0.198$, $q \simeq -0.98$, and the repelling black holes will have the mass $M \simeq 13.11$ and angular momentum $J \simeq 240.628$. On the other hand, from (8) and (9) it follows that the binary system of attracting black holes with the latter values of mass and angular momentum is characterized by $p \simeq -0.282$, $q \simeq 0.96$ and a considerably larger separation parameter $\kappa \simeq 33.075$. This result is logic if one recalls that the spin-spin repulsion force is inversely proportional to κ^4 [14] and hence decreases more rapidly with a larger distance than the gravitational force.

In the paper [6] it was observed that the stationary limit surface (SLS) of a solution with positive p has some features that distinguish it from the SLS of a solution with negative p . The main feature is of course the presence of a massless ring singularity outside the symmetry axis in the former solution, the appearance of which was attributed in [6] to the instabilities during the merging of SLSs. However, such an interpretation does not look quite precise in view of the intrinsic nature of the solutions with positive p established in the present paper – repelling black holes – and so we find it instructive in what follows to reexamine in more detail the geometrical properties of the solutions from the two subfamilies. For completeness, it is also desirable to study the issue of possible appearance of the regions with closed timelike curves (CTCs) attached to the massless ring singularities in order to evidence their benign character. To fulfil the latter objective we have obtained a very simple representation for the norm $\eta^\alpha \eta_\alpha$ of the axial Killing vector, namely,

$$\begin{aligned} \eta^\alpha \eta_\alpha &= \kappa^2 (x-1)(1-y^2)N/D, \\ N &= (x+1)(\mu+\nu)^2 - (x-1)(1-y^2)(x\sigma + \sigma - \tau)^2, \end{aligned} \quad (13)$$

whose negative values determine the regions with CTCs.

In Fig. 4 we have plotted the SLSs for the particular two solutions with $\delta_S = 1.4$ from the above example. The SLS in Fig. 4(a) belongs to the configuration of attracting extreme black holes separated by the coordinate distance $2\kappa \simeq 66.149$, and it does not have any massless ring singularity off the symmetry axis or a region of CTCs. In contrast, the SLS in Fig. 4(b) is accompanied by a massless ring singularity located in the equatorial plane, and also by a region of CTCs (inside the dotted curve) touching that singularity. It is clear that the extreme constituents in the second binary configuration are situated very close to each other, their SLSs having already formed a common SLS. However, since we have established that the black holes in Fig. 4(b) are repelling, it would be now plausible to infer that the ring singularity is not a product of merging of two SLSs, but rather a result of the beginning of desintegration of the common SLS into two parts.

Though the above analysis of Fig. 4 may look to provide a clear and simple description of how the attraction and repulsion of the extreme black holes work, the real situation with the interaction force is far more interesting and even puzzling. To see this, let us consider another two configurations of attracting and repelling black holes with the same separation parameter $\kappa = 2$ and angular-momentum–mass ratio $\delta_S = 1.99$, for which we readily find from (8) and (9) that the attracting constituents have the mass $M \simeq 13.978$ and angular momentum $J \simeq 388.792$, while

the mass and angular momentum of the repelling constituents are, respectively, $M \simeq 30.714$ and $J \simeq 1877.263$. In Fig. 5 we have plotted the SLSs of these binary systems, and it can be seen from Fig. 5(a) that the attracting extreme black holes have formed a common SLS, and neither a massless ring singularity nor a region of CTCs appear on that figure, which means that merging of the individual SLSs in that configuration has been realized through a smooth analytic process. At the same time, the SLS of repelling black holes depicted in Fig. 5(b), like earlier the SLS in Fig. 4(b), is accompanied by a massless ring singularity and by a region with CTCs, though it might look strange that the latter region is smaller than in Fig. 4(b) despite the larger angular momentum of the new system compared to the configuration in Fig. 4(b). However, a more exciting question would be about the binary systems in Figs. 4(b) and 5(a): the separation of extreme constituents in both systems is the same, so why do the black holes in Fig. 5(a) attract each other (instead of repelling) if their mass and the ratio δ_S are even larger than in the configuration from Fig. 4(b) and consequently are expected to produce a greater spin-spin repulsion effect?

Though a possible explanation for a smaller CTC region in Fig. 5(b) could be that the SLS of that configuration is only at the beginning of its splitting into two parts, while in Fig. 4(b) the division of the SLS is at a more advanced stage, the answer to the second question is not that simple and actually seems to be related to the recent findings of the paper [1]. First of all, Fig. 5(a) demonstrates that the unification of two SLSs can be a smooth process even at small separation distances and large values of mass, angular momentum and parameter δ_S approaching 2, so that the repulsion effect taking place in the configuration depicted in Fig. 4(b) should be basically attributed to instabilities of the SLS. However, the latter instabilities cannot be entirely explained by the SLS splitting due to repulsion of black holes alone, simply because an analogous repulsion does not take place inside the configuration from Fig. 5(a). Therefore, we inevitably arrive at the conclusion that the binary system from Fig. 4(b) represents a sort of a resonant state that produces instabilities of the SLS, as well as the configuration from Fig. 5(b). Such an inference looks plausible since a configuration of attracting black holes and a configuration of repelling black holes cannot have simultaneously the same particular values of M , J and κ , so that a resonant state producing the SLS instability occurs only when the latter characteristics of a binary system of extreme constituents all achieve the particular values belonging to the subfamily of repelling extreme black holes, i.e. a configuration with some admissible M and J must have a concrete parameter κ , a configuration with known M and κ – the concrete angular momentum J , and a configuration with some given J and κ – a special value of M for producing a resonant state and repulsion.

One of the sources of the SLS instability could be the nonuniqueness of the binary black-hole configurations characterized by the same mass and angular momentum of the constituents discovered in [1], because the SLS in this case must be affected by a possible spontaneous change of the multipole structure in such configurations. This sort of instability is certainly proper of the configuration from Fig. 5(b), which can be shown to belong to the so-called “triangle zone” of nonuniqueness [1, 15] giving rise to three different configurations of black holes: apart from the configuration of extreme black holes from Fig. 5(b), there are two other configurations of nonextreme identical black holes with the same mass $M \simeq 30.714$ and angular momentum $J \simeq 1877.263$ of the constituents, whose respective rescaled dimensionless quantities σ defining half-lengths of the horizons have been found to be $\sigma \simeq 0.215$ and $\sigma \simeq 0.175$.

At the same time, it is not difficult to check that the nonuniqueness argument is not applicable to the configuration of repelling extreme black holes from Fig. 4(b), as the latter does not belong to the nonuniqueness zone and hence there are no other binary configurations with the same mass, angular momentum and separation distance. The instability, notwithstanding, could be simply a result of a special, resonant status of the configuration itself which might produce perturbations of the SLS, and these in turn could give rise to the repulsion effect.

III. REPULSION OF TWO UNEQUAL EXTREME KERR BLACK HOLES

We now turn to consideration of the binary configurations of unequal extreme Kerr black holes generalizing the equatorially symmetric binary systems from the previous section. The Ernst complex potential \mathcal{E} defining this subfamily of the Kinnersley-Chitre solution has the form [6, 7]

$$\begin{aligned} \mathcal{E} &= (A - B)/(A + B), \\ A &= p^2 P^2 \{p^2(x^4 - 1) + q^2(y^4 - 1) - 2ixy[pq(x^2 - y^2) + \beta(x^2 + y^2 - 2)]\} \\ &\quad + [Q^2(p + q\beta)^2 - p^2 P^2 \beta^2](x^2 - y^2)^2 + 2ipPQ(p + q\beta)(x^2 + y^2 - 2x^2 y^2), \\ B &= 2pP(P - iQ)\{(x^2 - y^2)[pP\beta(qx + ipy) + Q(p + q\beta)(qy + ipx)] \\ &\quad + pP[p x(x^2 - 1) + i q y(y^2 - 1)]\}, \end{aligned} \tag{14}$$

where

$$\beta = \frac{p[P\Delta + q(1 + pP + Q^2)]}{2(p^2 - Q^2)}, \quad \Delta = \sqrt{4p^2(1 + pP) + q^2(p + P)^2}, \tag{15}$$

and the real parameters P and Q are subject to the same constraint as p and q : $P^2 + Q^2 = 1$.

The corresponding metric functions f , γ and ω , with a new form of ω , are given by the expressions

$$\begin{aligned}
f &= \frac{E}{D}, \quad e^{2\gamma} = \frac{E}{K_0^2(x^2 - y^2)^4}, \quad \omega = \frac{\kappa(x-1)(y^2-1)F}{E}, \\
E &= \mu^2 + (x^2 - 1)(y^2 - 1)\sigma^2, \\
D &= E + \mu\nu - (x-1)(y^2-1)\sigma\tau, \\
F &= (x+1)\sigma\nu + \mu\tau, \\
\mu &= p^2P^2[p^2(x^2-1)^2 + q^2(y^2-1)^2] + [Q^2(p+q\beta)^2 - p^2P^2\beta^2](x^2 - y^2)^2, \\
\sigma &= 2pP\{pP[pq(x^2 - y^2) + \beta(x^2 + y^2)] + 2Q(p+q\beta)xy\}, \\
\nu &= (4pP/K_0)\{K_0pP[pPx(x^2+1) + 2x^2 + qQy(y^2+1)] + K_0(x^2 - y^2) \\
&\quad \times [(p^2Q^2 + pq\beta)x + PQ(pq + \beta)y] - 2pP[q^2Q^2(p+q\beta)^2 + p^4P^2\beta^2](x^2 - y^2) \\
&\quad + 4p^2P^2(pq + \beta)x[pP\beta x + Q(p+q\beta)y]\}, \\
\tau &= \frac{4pP}{p^2 - q^2}\{pP(p^2 - q^2)(x+1)(qPx - pQy) + (p^2 - q^2)[(p^2 - Q^2)\beta - pq](x^2 - y^2) \\
&\quad - [(p^2 - Q^2)\beta - pq(1 + 2pP)](x+1)\}, \\
K_0 &= p^2P^2(p^2 - \beta^2) + Q^2(p+q\beta)^2,
\end{aligned} \tag{16}$$

and one can see that ω automatically vanishes at $y = \pm 1$ and $x = 1$ (see Fig. 1). The formulas for the total mass and total angular momentum of these binary configurations are

$$\begin{aligned}
M_T &= \frac{2\kappa p^2P(p+q\beta)}{p^2P^2(p^2 - \beta^2) + Q^2(p+q\beta)^2}, \\
J_T &= M \left[\frac{P(pq + \beta)M}{p+q\beta} - \frac{\kappa}{p} \left(qQ^2 - \frac{p^2P^2\beta}{p+q\beta} \right) \right],
\end{aligned} \tag{17}$$

while for the individual Komar masses and angular momenta of the constituents we have the expressions [7]¹

$$\begin{aligned}
M_1 &= \frac{\kappa[(q + pqP - p^2Q)\Delta - (1 + pP)(p + p^3 + q^2P - pqQ) + pq^3Q]}{2p(1 + pP)(p^2 - q^2)}, \\
M_2 &= \frac{\kappa[(q + pqP + p^2Q)\Delta - (1 + pP)(p + p^3 + q^2P + pqQ) - pq^3Q]}{2p(1 + pP)(p^2 - q^2)}, \\
J_1 &= \frac{(1 + pP + qQ)M_1^2}{2(p+P)^2} [(1 + pP + q^2)\Delta - 4pq + pq(p - P)^2], \\
J_2 &= \frac{(1 + pP - qQ)M_2^2}{2(p+P)^2} [(1 + pP + q^2)\Delta - 4pq + pq(p - P)^2],
\end{aligned} \tag{18}$$

and these were obtained as limits of the general expressions found by Tomimatsu [16] and Dietz and Hoenselaers [17] for the non-extended double-Kerr solution [4]. Note that J_1 and J_2 are given in the form most suitable for evaluating the individual angular-momentum–mass ratios $\delta_i = J_i/M_i^2$, $i = 1, 2$. The subindex 1 refers to the upper black hole and the subindex 2 to the lower black hole. As was observed in [7], J_1 and J_2 cannot have opposite signs, so the extreme constituents are corotating. Reduction to the case of two equal black holes occurs when $P = 1$, $Q = 0$.

The masses M_1 and M_2 take positive values, which are only of interest to us, for the following ranges of the parameters [7]:

$$-\frac{1}{\sqrt{2}} < p < 0, \quad q > 0; \quad -1 < P < -p \cup q < P < 1, \tag{19}$$

and

$$0 < p < \frac{1}{\sqrt{2}}, \quad q < 0; \quad -1 < P < q \cup -p < P < 1, \tag{20}$$

¹ We have rectified two misprints in the formulas (18) of [7]: the denominators of J_1 and J_2 should not have the factor p .

for arbitrary sign of Q . Comparing (19) with the negative values of p in (10), on the one hand, and (20) with the positive values of p in (10), on the other hand, one would anticipate that the subfamily of unequal black holes defined by (19) must describe attracting constituents, while the subfamily defined by (20) must describe the repelling constituents. The real situation is however a bit more complicated, as we shall see later on.

The expression for the interaction force between two unequal extreme Kerr constituents is obtainable from (11) and has the form

$$\mathcal{F} = \frac{p^2 P^2 (p^2 - q^2)}{4[p^2 P^2 (q^2 - \beta^2) + Q^2 (p + q\beta)^2]}, \quad (21)$$

and one can see that the sign of Q in the above expression for \mathcal{F} is irrelevant, unlike the sign of q . Note that the norm of the axial Killing vector in the case of unequal constituents is defined by the same simple formula (13) obtained in the previous section for identical black holes, but the quantities μ , ν , σ and τ entering it must be taken this time from (16).

The analysis of the interaction force (21) reveals that actually any of the subfamilies (19) or (20) may describe configurations of both attracting and repelling unequal extreme black holes. The case of attracting constituents in the subfamily (19) is defined by the positive values of P on the interval $P \in (q, 1)$, while in the subfamily (20) such configurations correspond to negative P on the interval $P \in (-1, q)$, and these are of no interest to us. The configurations of repelling constituents arise in the subfamily (19) at $P \in (-1, -p)$, and in the subfamily (20) at $P \in (-p, 1)$, the latter two intervals containing both positive and negative values of P . Apparently, the case of unequal constituents provides more possibilities for the extreme black holes to repel each other, and the individual angular-momentum–mass ratios δ_i of the repelling unequal constituents may exceed significantly the respective maximum value 2 of identical black holes. Restricting ourselves to the repulsion of unequal black holes, in Figs. 6 and 7 we have depicted the SLSs, the regions with CTCs and massless ring singularities for the binary configurations defined by the same values of κ , p and q as in Figs. 4 and 5 but different values of P and Q (we recall that for the identical black holes $P = 1$, $Q = 0$). Thus, in Fig. 6(a) the values of κ , p and q defining the system of repelling black holes are the same as in Fig. 4(b), but with $P = 0.5$, $Q \simeq 0.866$. The masses of black holes are $M_1 \simeq 9.918$ and $M_2 \simeq 6.194$, and the corresponding individual angular-momentum–mass ratios are $\delta_1 \simeq 0.618$ and $\delta_2 \simeq 4.812$ (we give them instead of the angular momenta of the constituents); though the splitting of the common SLS into two disconnected parts has already occurred, a byproduct of that non-smooth process is the appearance of the third separate component of SLS that characterizes the instability zone marked by the massless ring singularity and associated region of CTCs. The interaction force $\mathcal{F} \simeq -0.2493$, hence being repulsive, and the binary system as a whole looks to a distant observer as a subextreme object because $\delta_T \equiv J_T/M_T^2 \simeq 0.945$.

The configuration from the subfamily (19) whose SLS is plotted in Fig. 6(b) is defined by the same particular values of κ , p and q as the configuration of attracting constituents in Fig. 4(a), but its P and Q are different: $P = -0.8$, $Q = 0.6$, which leads to the repulsion of the constituents since $\mathcal{F} \simeq -0.2487$. The above change of P and Q affects drastically the masses of black holes, yielding $M_1 \simeq 130.589$ and $M_2 \simeq 176.792$, together with the angular-momentum–mass ratios $\delta_1 \simeq 2.776$ and $\delta_2 \simeq 1.001$; at the same time, $\delta_T \simeq 0.832$ which is characteristic of a subextreme object, as in the previous example. The presence of a massless ring singularity and associated region of CTCs is an indication that there is a zone of instability due to disintegration of the common SLS.

The plots given in the next Figs. 7(a) and 7(b) are very similar, despite representing configurations from different subfamilies (19) and (20). Both configurations are composed of repelling black holes, have large SLSs and small instability zones accompanied by massless ring singularities and regions of CTCs. The configuration from Fig. 7(a) shares the same values of κ , p and q with the configuration from Fig. 5(b), but its P and Q are different: $P = 0.2$, $Q \simeq 0.98$. The individual masses M_i and ratios δ_i of the constituents are $M_1 \simeq 34.699$, $M_2 \simeq 9.04$, $\delta_1 \simeq 1.195$ and $\delta_2 \simeq 5.811$, so that the ratio δ_T involving total mass and total angular momentum becomes $\delta_T \simeq 1.00042$, and the binary system looks to a distant observer as a hyperextreme object. On the other hand, the values of κ , p and q of the configuration from Fig. 7(b) are the same as for the configuration from Fig. 5(a), the remaining two parameters having the values $P = -0.8$ and $Q = 0.6$; the masses of the constituents are $M_1 \simeq 29.431$ and $M_2 \simeq 50.172$, and the corresponding angular-momentum–mass ratios are $\delta_1 \simeq 2.814$ and $\delta_2 \simeq 1.545$, the ratio δ_T of this configuration being equal to 0.998. These examples clearly demonstrate that the configurations of unequal extreme black holes lend more opportunities for their constituents to repel each other than the binary systems comprised exclusively of identical black holes.

IV. DISCUSSION AND CONCLUSIONS

Therefore, we have shown that there are vast families of binary configurations of repelling extreme Kerr black holes endowed with positive masses. The repulsion effect arises due to spin-spin interaction of the constituents when a

binary system achieves a specific state, which we tentatively call “resonant”, characterized by instabilities of the SLS. Such instabilities seem to be mainly determined by the disintegration of the common SLS into two or more fragments through a non-smooth process, but could also be an intrinsic characteristic and inseparable part of the resonant states themselves, somehow contributing to the repulsion of black holes too. In our analysis we have put emphasis on the geometrical characteristics of the repelling extreme black holes such as SLSs, massless ring singularities and regions with CTCs in order to elucidate an important role of the latter two in maintaining the stationarity of the configurations and to justify their benign character. Since historically the massless ring singularities puzzled the researchers for quite a long time, in what follows we would like to make a few additional comments on them.

While the physical significance of massless struts (conical singularities) was understood long ago [10, 11] and the presence of struts in the two-body solutions of general relativity is considered as “a very satisfactory feature of this nonlinear theory” [18], the massless ring singularities were first reported by far later in relation to the Tomimatsu-Sato solutions [19] and were commonly regarded, together with the associated regions of CTCs, as some undesirable pathological characteristics of spacetimes [20]. It was conjectured by Hoenselaers [21] that in the multi-black-hole configurations a constituent with negative mass should be accompanied by a naked singularity, and in the paper [22] it was demonstrated that the massless ring singularity in $\delta = 2$ Tomimatsu-Sato solution is linked to a region of negative mass existing in that solution. Examples of appearance of ring singularities in the spacetimes involving negative mass were also given in the framework of extended double-Kerr solution [3], so that one might think in principle that a naked singularity is a proper intrinsic feature of *any* negative mass and then call “unphysical” both the massless ring singularity and the negative mass (what usually happens).

However, the discovery of the binary black-hole configurations involving exclusively positive masses and yet having ring singularities outside the symmetry axis, such as the ones considered in [1, 6, 7], urges us to make a more profound and broader look at the massless ring singularities in order to bring to light the universal task they fulfil in the stationary axisymmetric spacetimes. Taking into account that the Schwarzschild and Kerr solutions endowed with negative mass are known to be unstable [23, 24], and also that a massless ring singularity arising in the configurations of interacting black holes carrying positive masses can be associated with the instabilities of SLSs, it would be plausible to suppose that the unique function such singularities perform in stationary spacetimes is simply maintaining the stationarity of the latter, which is actually the same role as performed by the conical singularities, but covering more situations where the instabilities may occur. In this respect, it is clear that the ring singularities and associated regions of CTCs in the configurations of repelling black holes considered in the previous sections are needed to detain the dynamical evolution of SLSs which would otherwise go on changing their shapes despite the unchanging positions of black holes on the symmetry axis ensured by struts. It should be emphasized that in the real axisymmetric nonstationary configurations of interacting extreme black holes which are mimicked by our stationary solutions, neither the struts on the axis nor the ring singularities off the axis of symmetry will be present because the evolution of the black holes and SLSs then will not be artificially constrained by the stationarity condition. As a result, the repelling constituents will be moving away from each other and the SLSs will be changing their aspect in a natural, unrestricted way, the dynamical evolution being also accompanied by a small loss of energy in the form of gravitational waves [25].

Lastly, it is tempting to speculate that the observational phenomenon of recoiling black holes [26, 27] which the astronomers attribute so far to the powerful gravitational radiation liberated during the merging process, could be just a natural outcome of the spin-spin interaction of corotating black holes during the head-on collision.

Acknowledgments

This work was supported in part by the CONACYT of Mexico, and by Project FIS2015-65140-P (MINECO/FEDER) of Spain. One of us (VSM) would like to thank the Department of Quantum Statistics and Field Theory of the Moscow State University for the hospitality extended to him during his visit there in July 2018.

-
- [1] V. S. Manko and E. Ruiz, “Black hole-naked singularity” dualism and the repulsion of two Kerr black holes due to spin-spin interaction, *Phys. Lett. B* **791**, 26 (2019).
 - [2] V. S. Manko and E. Ruiz, Extended multi-soliton solutions of the Einstein field equations, *Class. Quantum Grav.* **15**, 2007 (1998).
 - [3] V. S. Manko, E. Ruiz and J. D. Sanabria-Gómez, Extended multi-soliton solutions of the Einstein field equation: II. Two comments on the existence of equilibrium states, *Class. Quantum Grav.* **17**, 3881 (2000).
 - [4] D. Kramer and G. Neugebauer, The superposition of two Kerr solutions, *Phys. Lett. A* **75**, 259 (1980).
 - [5] W. Kinnersley and D. M. Chitre, Symmetries of the Einstein-Maxwell equations. IV. Transformations which preserve asymptotic flatness, *J. Math. Phys.* **19**, 2037 (1978).

- [6] V. S. Manko and E. Ruiz, On a simple representation of the Kinnersley-Chitre metric, *Prog. Theor. Phys.* **125**, 1241 (2011).
- [7] V. S. Manko, E. Ruiz, and M. B. Sadovnikova, Stationary configurations of two extreme black holes obtainable from the Kinnersley-Chitre solution, *Phys. Rev. D* **84**, 064005 (2011).
- [8] R. P. Kerr, Gravitational field of a spinning mass as an example of algebraically special metrics, *Phys. Rev. Lett.* **11**, 237 (1963).
- [9] F. J. Ernst, New formulation of the axially symmetric gravitational field problem, *Phys. Rev.* **167**, 1175 (1968).
- [10] R. Bach and H. Weyl, Neue Lösungen der Einsteinschen Gravitationsgleichungen, *Math. Z.* **13**, 134 (1922).
- [11] W. Israel, Line sources in general relativity, *Phys. Rev. D* **15**, 935 (1977).
- [12] A. Komar, Covariant conservation laws in general relativity, *Phys. Rev.* **113**, 934 (1959).
- [13] G. Weinstein, On rotating black holes in equilibrium in general relativity, *Comm. Pure Appl. Math.* **43**, 903 (1990).
- [14] R. Wald, Gravitational spin interaction, *Phys. Rev. D* **6**, 406 (1972).
- [15] V. S. Manko and E. Ruiz, Metric for two equal black holes, *Phys. Rev. D* **96**, 104016 (2017).
- [16] A. Tomimatsu, On gravitational mass and angular momentum of two black holes in equilibrium, *Prog. Theor. Phys.* **70**, 385 (1983).
- [17] W. Dietz and C. Hoenselaers, Two mass solutions of Einstein's vacuum equations: The double Kerr solution, *Ann. Phys. (NY)* **165**, 319 (1985).
- [18] H. Stephani, D. Kramer, M. MacCallum, C. Hoenselaers, and E. Herlt, *Exact Solutions of Einstein's Field Equations* (Cambridge: Cambridge University Press, 2003) p. 307.
- [19] A. Tomimatsu and H. Sato, New exact solution for the gravitational field of a spinning mass, *Phys. Rev. Lett.* **29**, 1344 (1972).
- [20] G. W. Gibbons and R. A. Russell-Clark, Note on the Sato-Tomimatsu solution of Einstein's equations, *Phys. Rev. Lett.* **30**, 398 (1973).
- [21] C. Hoenselaers, Remarks on the double-Kerr solution, *Prog. Theor. Phys.* **72**, 761 (1984).
- [22] V. S. Manko, On the physical interpretation of $\delta = 2$ Tomimatsu-Sato solution, *Prog. Theor. Phys.* **127**, 1057 (2012).
- [23] R. J. Gleiser and G. Dotti, Instability of the negative mass Schwarzschild naked singularity, *Class. Quantum Grav.* **23**, 5063 (2006).
- [24] V. Cardoso and M. Cavaglià, Stability of naked singularities and algebraically special modes, *Phys. Rev. D* **74**, 024027 (2006).
- [25] S. Dain and O. E. Ortiz, Numerical evidences for the angular momentum-mass inequality for multiple axially symmetric black holes, *Phys. Rev. D* **80**, 024045 (2009).
- [26] S. Komossa, H. Zhou, and H. Lu, A recoiling supermassive black hole in the quasar SDSS J092712.65+294344.0? *Astrophys. J.* **678**, L81 (2008).
- [27] L. Blecha, D. Sijacki, L. Z. Kelley, *et al*, Recoiling black holes: prospects for detection and implications of spin alignment, *Mon. Not. R. Astron. Soc.* **456**, 961 (2016).

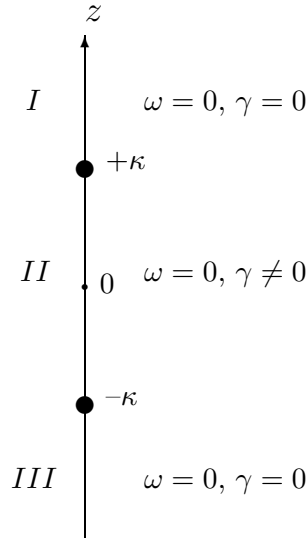


FIG. 1: Location of two extreme black holes on the symmetry z -axis (at the points $z = \pm\kappa$), and behavior of the metric functions ω and γ on three different parts of the symmetry axis: $z > \kappa$ (part *I*), $-\kappa < z < \kappa$ (part *II*) and $z < -\kappa$ (part *III*).

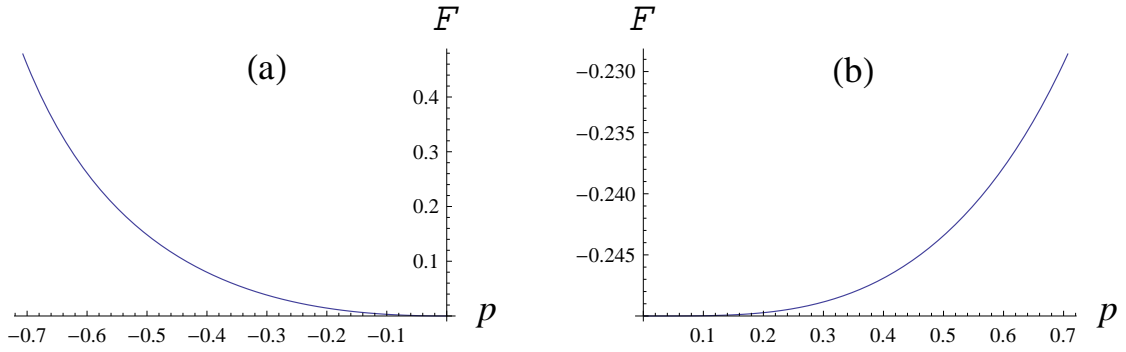


FIG. 2: Interaction force \mathcal{F} for two subfamilies of equal extreme Kerr black holes: (a) the case of attracting black holes ($-1/\sqrt{2} < p < 0, q > 0$), (b) the case of repelling black holes ($0 < p < 1/\sqrt{2}, q < 0$).

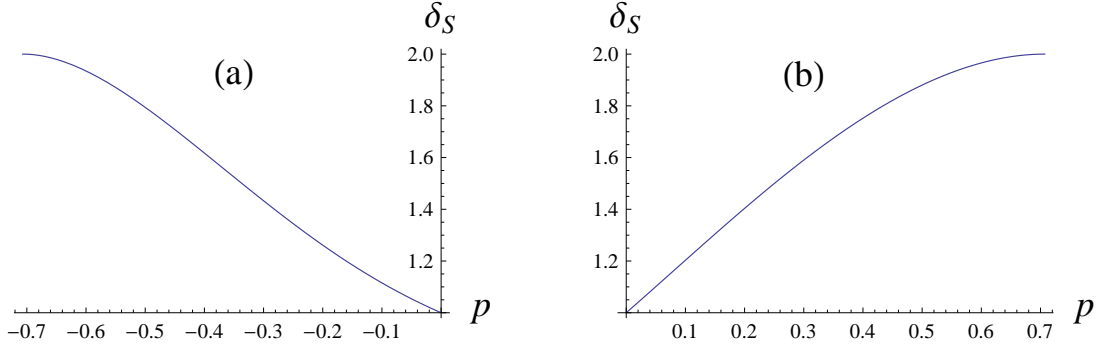


FIG. 3: Plot of the angular-momentum–mass ratio $\delta_S(p)$ for two subfamilies of equal extreme Kerr black holes from section II: (a) the case of attracting black holes; (b) the case of repelling black holes. For both subfamilies, δ_S runs the values on the interval $(1, 2)$.

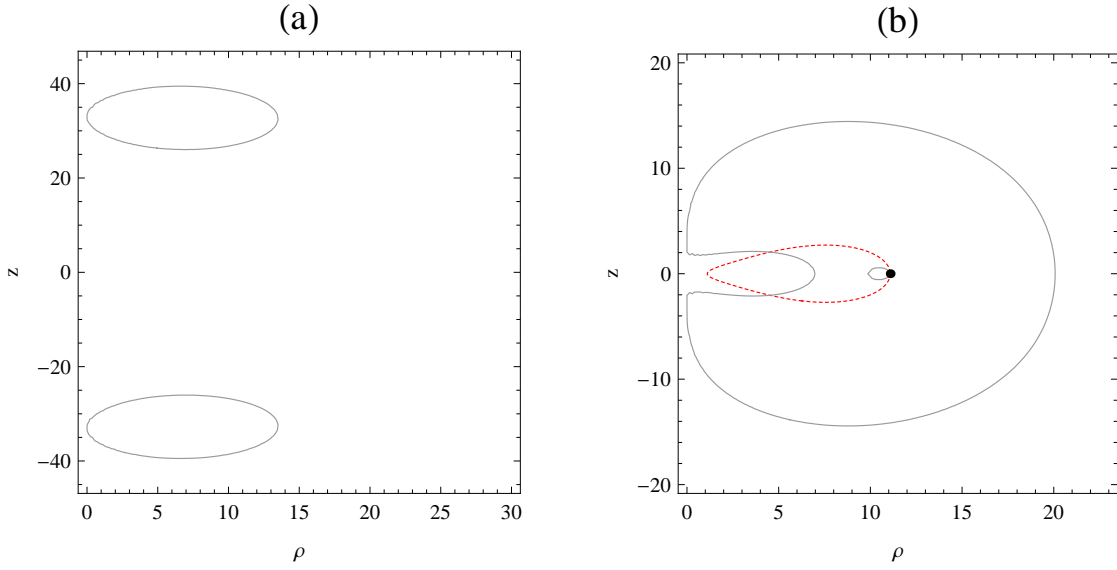


FIG. 4: The SLSs for two different binary configurations of extreme Kerr black holes that have the same masses and angular momenta ($M \simeq 13.11$ and $J \simeq 240.628$): (a) the attracting black holes located at $\kappa \simeq \pm 33.075$ which do not develop a massless ring singularity or the region of CTCs; (b) the repelling black holes located at $\kappa = \pm 2$ which develop a massless ring singularity (at $z = 0$, $\rho \simeq 11.081$) and the region with CTCs (inside the dotted curve), thus indicating that the common SLS tends to be divided into two separate parts.

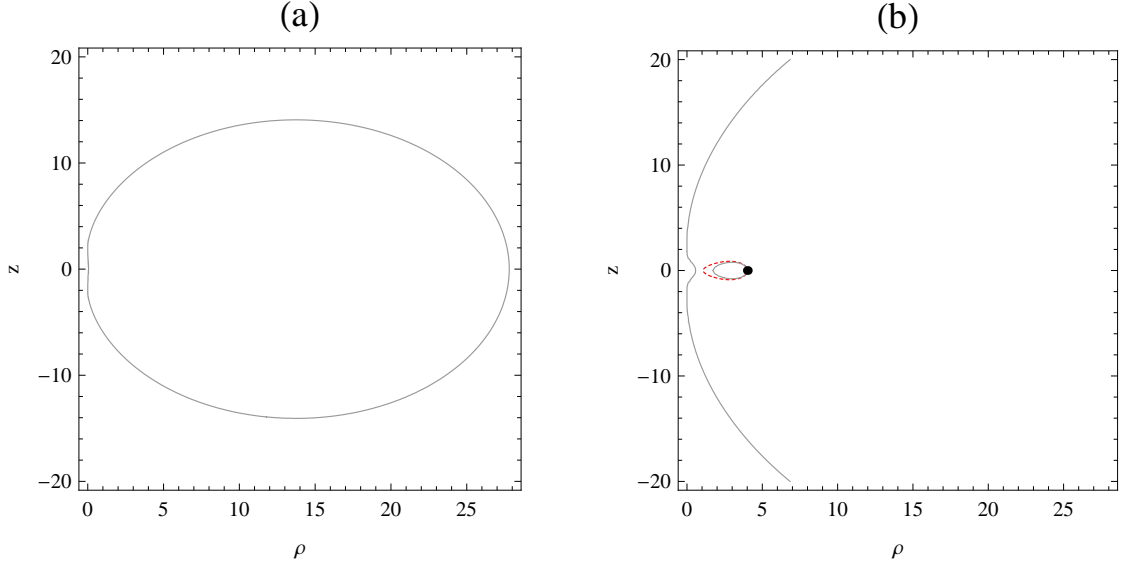


FIG. 5: The SLSs for two binary configurations of extreme Kerr black holes located at $\kappa = \pm 2$ and characterized by the same ratio $\delta_S = 1.99$: (a) the individual mass and angular momentum of attracting black holes are $M \simeq 13.978$ and $J \simeq 388.792$, respectively, a massless ring singularity off the symmetry axis and the region of CTCs are absent; (b) the repelling black holes have individual mass $M \simeq 30.714$ and angular momentum $J \simeq 1877.263$ and develop a massless ring singularity at $z = 0$, $\rho \simeq 4.007$, accompanied by a region of CTCs.

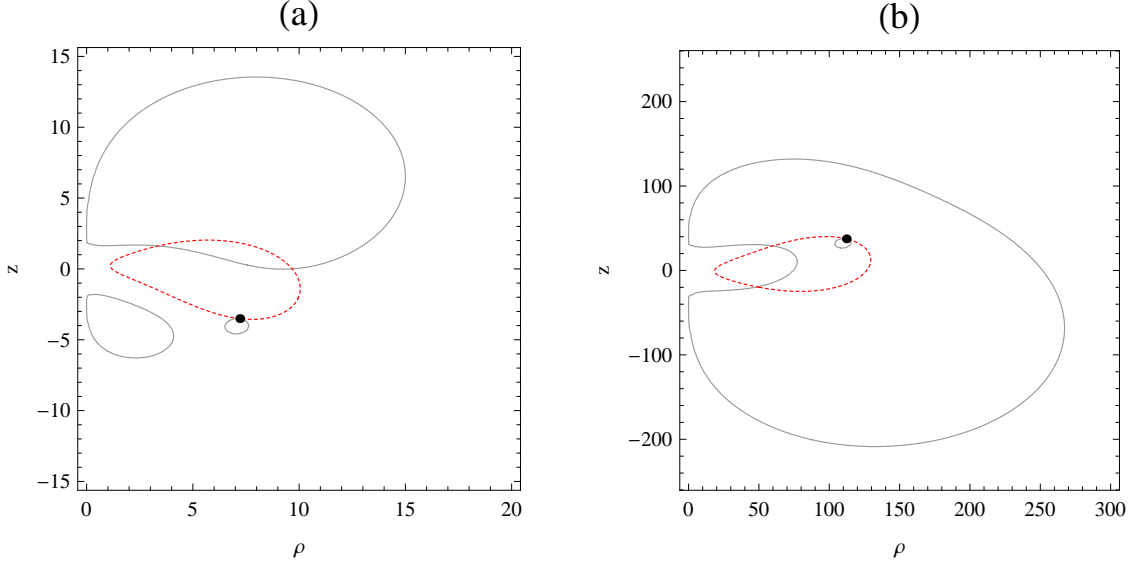


FIG. 6: The SLSs for two binary configurations of repelling extreme unequal black holes defined by the same values of the parameters κ , p and q as in Fig. 4: (a) a configuration from the subfamily (20) with $P = 0.5$, $M_T \simeq 16.112$ and $\delta_T \simeq 0.945$; the massless ring singularity is located at $\rho \simeq 7.209$, $z \simeq -3.508$, (b) a binary system from the subfamily (19) with $P = -0.8$, $M_T \simeq 307.381$ and $\delta_T \simeq 0.832$; the massless ring singularity is located at $\rho \simeq 112.126$, $z \simeq 37.431$.

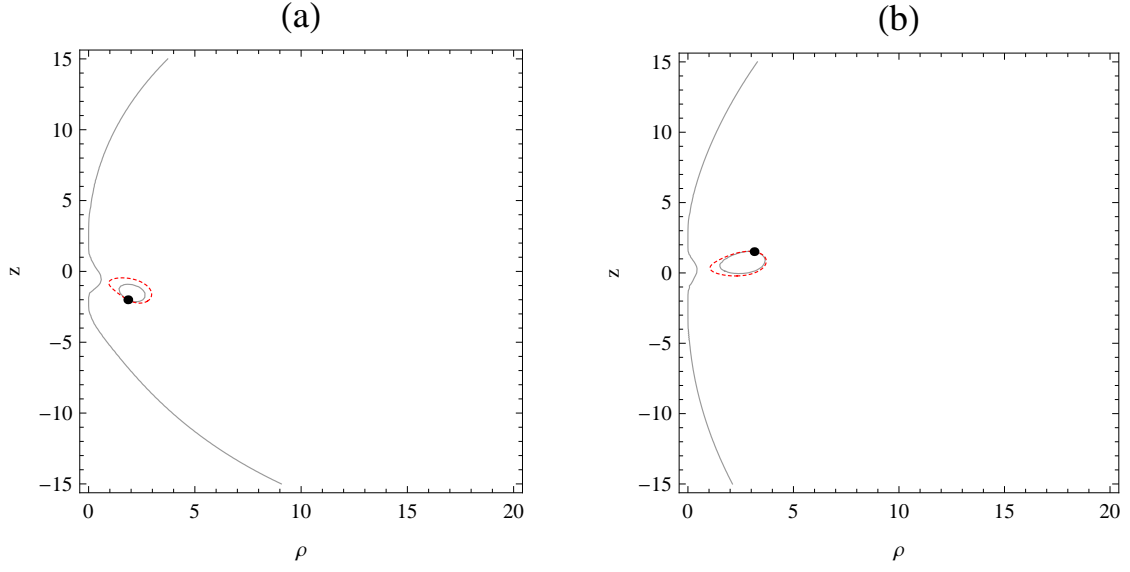


FIG. 7: The SLSs for two binary configurations of repelling extreme unequal black holes defined by the same values of the parameters κ , p and q as in Fig. 5: (a) a configuration from the subfamily (20) with $P = 0.2$, $M_T \simeq 43.74$ and $\delta_T \simeq 1.00042$; the massless ring singularity is located at $\rho \simeq 1.845$, $z \simeq -2.004$, (b) a binary system from the subfamily (19) with $P = -0.8$, $M_T \simeq 79.603$ and $\delta_T \simeq 0.998$; the massless ring singularity is located at $\rho \simeq 3.135$, $z \simeq 1.512$.